



# Association of Increased Amygdala Activity with Stress-Induced Anxiety but not Social Avoidance Behavior in Mice

Shou-He Huang<sup>1</sup> · Wei-Zhu Liu<sup>1</sup> · Xia Qin<sup>1</sup> · Chen-Yi Guo<sup>1</sup> · Qing-Cheng Xiong<sup>1</sup> · Yu Wang<sup>1</sup> · Ping Hu<sup>2</sup> · Bing-Xing Pan<sup>1</sup> · Wen-Hua Zhang<sup>1</sup>

Received: 19 January 2021 / Accepted: 16 May 2021 / Published online: 7 September 2021  
© Center for Excellence in Brain Science and Intelligence Technology, Chinese Academy of Sciences 2021

**Abstract** Chronic stress leads to many psychiatric disorders, including social and anxiety disorders that are associated with over-activation of neurons in the basolateral amygdala (BLA). However, not all individuals develop psychiatric diseases, many showing considerable resilience against stress exposure. Whether BLA neuronal activity is involved in regulating an individual's vulnerability to stress remains elusive. In this study, using a mouse model of chronic social defeat stress (CSDS), we divided the mice into susceptible and resilient subgroups based on their social interaction behavior. Using *in vivo* fiber photometry and *in vitro* patch-clamp recording, we showed that CSDS persistently (after 20 days of recovery from stress) increased BLA neuronal activity in all the mice regardless of their susceptible or resilient nature, although impaired social interaction behavior was only observed in susceptible mice. Increased anxiety-like behavior, on the other hand, was evident in both groups. Notably, the CSDS-induced increase of BLA neuronal activity correlated well with the heightened anxiety-like but not the social avoidance behavior in mice. These findings provide new insight to our understanding of the role of neuronal activity in the amygdala in mediating stress-related psychiatric disorders.

**Keywords** Chronic stress · Amygdala · Stress vulnerability · Anxiety · Fiber photometry · Neuronal activity

## Introduction

Exposure to chronic stress increases the risk of developing psychopathology, including anxiety disorder and major depressive disorder [1–4]. Stressful life events are unavoidable throughout the lifespan; however, the occurrence of psychiatric disorders varies across individuals when they are exposed to the same extreme stress. While most people recover from stressful events and show considerable resilience, nearly 20% are vulnerable to such events and thus develop stress-related disorders [5–8]. In this context, it appears urgent to understand the brain mechanisms governing stress resilience and vulnerability, as they are a prerequisite for the development of new therapeutic approaches to psychopathologies associated with stress.

Social defeat stress during adolescence is one of the critical factors affecting the onset of depressive disorders in humans [9]. The mouse model of chronic social defeat stress (CSDS) has been widely used to explore the mechanisms underlying stress-related behaviors [5, 10]. In this model, the mice are subjected to multiple episodes of social defeat stress, and their vulnerability to stress is then defined according to their performance in a social interaction (SI) test. The mice that display avoidance behavior to the social stressor in this test are defined as susceptible, and this group of mice also show anhedonia and despair behavior, which are key symptoms of depression. By contrast, the mice not showing such behaviors after stress are identified as resilient [5]. In the past decade, this excellent model has helped to markedly expand our understanding of the neural substrates underlying stress

Shou-He Huang and Wei-Zhu Liu have contributed equally to this work.

✉ Bing-Xing Pan  
panbingxing@ncu.edu.cn

✉ Wen-Hua Zhang  
whzhang@ncu.edu.cn

<sup>1</sup> Laboratory of Fear and Anxiety Disorders, Institutes of Life Science, Nanchang University, Nanchang 330031, China

<sup>2</sup> Institute of Translational Medicine, Nanchang University, Nanchang 330001, China

susceptibility and resilience [10, 11]. For example, researchers have demonstrated the roles of various neurotransmitters, hormones, and neuropeptides, as well as multiple genetic factors in the neurobiology of resilience [12]. Nevertheless, understanding of the neurobiological differences between susceptible and resilient individuals is rather limited.

The mechanisms underlying coping with stress are associated with neurobiological changes in several brain regions [13, 14]. Among them, the amygdala, a kernel area for the expression of mood and emotion, has been strongly implicated in both the physiological and pathological responses to stress [15–17]. Many studies have demonstrated that aberrant neuronal activity and hyperexcitability in the amygdala are critically engaged in the occurrence of a series of stress-related psychiatric disorders, such as social disorder [3] and anxiety disorder [18]. In the resting state, the amygdala is under the tight control of strong inhibitory tone, which limits its excessive activation and is essential for the maintenance of a normal emotional state as well as the avoidance of inappropriate responses to external stimuli [19]. However, under exposure to stress, the inhibitory tone in the amygdala is removed, and its neurons become disinhibited and hyperexcited. The increased activity of the amygdala, especially its basolateral part (BLA), drives increased emotional output and contributes to a spectrum of stress-related psychiatric disorders [20–23]. Notably, most of the information is from studies focusing on the detection of BLA neuronal activity at a specific time point after stress exposure. How the BLA neurons show dynamic changes to stress and contribute to stress vulnerability remains largely unknown.

Recently, the fiber photometry system has attracted wide interest due to its convenience, sensitivity, and reliability in dynamically monitoring  $\text{Ca}^{2+}$  signals under designed behavioral paradigms in freely-moving mice [24–27]. It also effectively avoids electromagnetic noise and interfering physiological activity. In this study, with the aid of fiber photometry, we recorded the dynamic activity of BLA neurons responding to CSDS and explored their role in regulating the susceptibility to stress-related psychiatric disorders. We also used *in vitro* electrophysiology to test the effects of CSDS on BLA neurons. Finally, we analyzed the correlation between CSDS-induced changes of BLA neuronal activity and its effects on mice's stress-related behavior.

## Materials and Methods

### Animals

Male C57BL/6J mice (4 or 7 weeks old) were used in all experiments. They were maintained in a temperature- and humidity-controlled room with a light/dark cycle of 12-h (lights on 07:00, off 19:00) and *ad libitum* access to food and water. All experimental procedures were performed following the guidelines of the National Institutes of Health and approved by the Institutional Animal Care and Use Committee of Nanchang University.

### Chronic social defeat stress and the social interaction test

CSDS was imposed as previously described [28, 29]. Briefly, we screened CD1 retired breeder mice aged 4–6 months for aggressive behavior upon intrusion into their home cages. Those exhibiting aggression were used to defeat C57BL/6J mice. During CSDS, a male C57BL/6J mouse (test mouse, 7 weeks old) was exposed to a different CD1 aggressor mouse (target mouse) for 5 min each day for 10 consecutive days. After the defeat episodes, the test mouse was separated from an aggressor by a perforated acrylic barrier where it was persistently exposed to the threat for the next 24 h. Each control mouse was gently handled every day and housed opposite another C57BL/6J mouse. In the SI test, the C57BL/6J mouse was placed in a square open-field arena with a small animal cage at one end, and its movement was tracked for 5 min in two 2.5-min epochs. The time spent in the interaction zone during the first (target absent) and second (target present) epoch was measured. The SI ratio was calculated as (Interaction time with CD1 present)/(Interaction time with CD1 absent)  $\times$  100%. ANY-maze 6.3 (Stoelting Co., USA) was used to analyze the times in the interaction and corner zones. Mice with an SI ratio  $<100\%$  were considered susceptible (SI-sus), and those with an SI ratio  $\geq 100\%$  were considered resilient (SI-res).

### Open Field Test (OFT)

The open field chamber was made of transparent plastic (50 cm  $\times$  50 cm) and a 25 cm  $\times$  25 cm center square was defined as the center area. Each mouse was placed in the center of the chamber before starting the 10-min session. An overhead video-tracking system (Med Associates Inc., Fairfax, VT) was used to monitor their behavior. Time in the center area and total distance traveled were analyzed by the ANY-maze 6.3 software (Stoelting Co., USA).

Following each trial, the apparatus was cleaned with 70% ethanol to remove olfactory cues.

### Elevated Plus Maze (EPM) Test

Six hours after the OFT test, the mice were subjected to the EPM test. The EPM apparatus consisted of two open arms (35 cm × 6 cm), two closed arms (35 cm × 6 cm), and a central connecting platform (6 cm × 6 cm). The apparatus was elevated 74 cm above the floor. Each mouse was placed on the central platform, facing an open arm, followed by 10-min monitoring of its behavior using the video-tracking system (Med Associates Inc.). The ANY-maze 6.3 software was used to analyze the time spent in the open arms and entries into the open or closed arms. After each trial, the apparatus was cleaned with 70% ethanol to remove olfactory cues.

### Fiber Photometry

Four-week-old mice were anesthetized with 5% isoflurane in a clean induction chamber and head-fixed in a stereotaxic frame (RWD, Shenzhen, China). Anesthesia was maintained *via* delivery of 1%–2% isoflurane during surgical procedures. Body temperature was maintained with a heat lamp. We injected 0.3 μL of AAV-CaMKIIα-GCaMP6s or AAV-CaMKIIα-EGFP virus (Obio Technology, Shanghai, China) into the BLA (bregma coordinates: anterior/posterior, −1.3 mm; medial/lateral, +3.15 mm; dorsal/ventral, −5.05 mm) at 80 nL/min, and a 200-μm diameter optical fiber was immediately implanted into the BLA (dorsal/ventral, −5 mm). Three weeks after surgery, the mice were subjected to the SI test with concurrent recording of the GCaMP6s signal. The GCaMP6s fluorescence was recorded by a fiber photometry system (Thinker Tech Nanjing Biotech Limited Co., Ltd). To induce GCaMP6s fluorescence, 488-nm laser light was delivered using the fiber photometry system, and fluorescent signals were recorded. In data analysis, to normalize the fluorescent signal data from each mouse, the changes of Ca<sup>2+</sup> signal values were calculated as:  $(\Delta F/F) = (F - F_0)/F_0$ , where  $F_0$  is the average baseline Ca<sup>2+</sup> signal during a 2-s control time-window prior to a defined event. For the acute stress assay, the data are presented as heatmaps or as peri-event plots with a shaded area indicating the SEM, and as histograms of the  $\Delta F/F$  average values that include 2 s before and 5 s after a CD1 mouse attack. For the chronic stress assay, the peak  $\Delta F/F$  value in a 5-s window centered on the defined behavioral event (proximal interaction toward enclosure) was identified and the peak values were compared across groups. Since the number of interaction zone entries and proximal interactions differed between the SI-sus and SI-res mice, to ensure comparability, only the

first incidence of each event was included. All data were analyzed with MatLab R2016b (The MathWorks).

### Histology and Microscopy

Histology and microscopy experiments were performed as previously described with minor modifications [30, 31]. Briefly, mice were anesthetized with 2% sodium pentobarbital, followed by transcardial perfusion with phosphate-buffered saline (PBS) and 4% paraformaldehyde (PFA) successively to fix the tissues. The brains were post-fixed overnight at 4°C in 4% PFA. Coronal slices were cut on a VT1200S vibratome (Leica Microsystems). Subsequently, the slices were incubated for 5 min with 4',6-diamidino-2-phenylindole, a DNA-specific fluorescent probe, rinsed in PBS (3 × 5 min), and mounted with fluoromount aqueous mounting medium (Sigma-Aldrich, Saint Louis, MO, USA). Images were captured with the Virtual Slide System (VS120; Olympus Corp., Tokyo, Japan).

### Amygdala Slice Preparation

Amygdala slices were prepared as described previously [28, 30]. Briefly, mice were deeply anesthetized decapitated, and the brains were removed immediately and chilled in ice-cold cutting solution containing (in mmol/L) 80 NaCl, 3.5 KCl, 4.5 MgSO<sub>4</sub>, 0.5 CaCl<sub>2</sub>, 1.25 NaH<sub>2</sub>PO<sub>4</sub>, 25 NaHCO<sub>3</sub>, 90 sucrose, and 10 glucose, aerated with 95% O<sub>2</sub> and 5% CO<sub>2</sub>. The 320-μm thick coronal slices containing the amygdala were cut on the VT1200S vibratome (Leica Microsystems), allowed to recover in artificial cerebrospinal fluid (ACSF) containing (in mmol/L): 124 NaCl, 2.5 KCl, 2 MgSO<sub>4</sub>, 2.5 CaCl<sub>2</sub>, 1.25 NaH<sub>2</sub>PO<sub>4</sub>, 22 NaHCO<sub>3</sub>, and 10 glucose, for 30 min at 34°C, and then transferred to a holding chamber with ACSF (bubbled with 95% O<sub>2</sub> and 5% CO<sub>2</sub>) for at least 1 h at room temperature before recording.

### Whole-Cell Patch-Clamp Recordings

Whole-cell patch-clamp recordings were performed as previously described [31]. Briefly, a single slice containing the amygdala was transferred to the recording chamber under continuous perfusion with ACSF (1 mL/min–2 mL/min). Patch electrodes were made from filamented borosilicate glass capillary tubes (inner diameter, 0.84 μm) using a horizontal pipette puller (P97, Sutter Instrument, Novato, CA, USA). To record action potentials (APs) in BLA projection neurons (PNs), patch electrodes with a resistance of 3 MΩ–7 MΩ were filled with an internal solution containing (in mmol/L): 130 K-gluconate, 5 NaCl, 1 MgCl<sub>2</sub>, 10 HEPES, 0.2 EGTA, 0.1 NaGTP, and 2 MgATP,

pH adjusted to 7.3 and osmolarity to 285 mOsm. Then, 20  $\mu\text{mol/L}$  CNQX and 100  $\mu\text{mol/L}$  picrotoxin were added to the bath solution. Cells were recorded in current-clamp mode, and depolarizing current pulse ramps (250 pA over 1.5 s) or increasing in steps of 50 pA (0 pA–250 pA, 1 s) were injected. A junction potential of  $\sim 12$  mV was not corrected. The data were discarded if the series resistance changed by  $>20\%$ .

### Statistical Analyses

All the data are shown as the mean  $\pm$  SEM. The statistical analyses were performed using GraphPad Prism 7 (GraphPad Software, Inc., San Diego, CA) or SPSS 19.0 (SPSS Inc., Chicago, IL, USA), using one-way and two-way ANOVA with or without repeated measures, followed by *post-hoc* comparisons with Bonferroni's test. The homogeneity of variance and normality were analyzed with Levene's test and the Kolmogorov–Smirnov test, respectively. If these assumptions were violated, the Wilcoxon signed-rank test or Mann-Whitney test were applied where appropriate. Pearson's correlation and linear regression analysis were used to evaluate correlations.  $P < 0.05$  was considered statistically significant.

## Results

### Defeat Stress Rapidly Increases Neuronal Activity in the BLA

We investigated the dynamic changes of BLA neural activity in freely-moving awake mice during defeat stress exposure (social attack) using *in vivo* fiber photometry (Fig. 1A). To this end, a genetically encoded  $\text{Ca}^{2+}$  indicator, GCaMP6s, was expressed in the BLA PNs by injecting AAV-CaMKII $\alpha$ -GCaMP6s or AAV-CaMKII $\alpha$ -EGFP into the BLA (Fig. 1B), where an optical fiber was implanted (Fig. 1C). The tested mice were placed in the home cage of an aggressive male CD1 aggressor, where they were frequently attacked by the CD1 mouse. The changes in GCaMP6s fluorescence, which reflect real-time neuronal activity, were monitored through the optical fiber embedded in the BLA during the entire process of stress exposure.

We first found that the  $\text{Ca}^{2+}$  signals in the tested mice expressing GCaMP6s robustly increased when they were attacked by a CD1 mouse, while in mice expressing EGFP, the signals remained unaltered during attacks (Fig. 1D), indicating that the signals were indeed derived from defeat stress-evoked changes in cellular  $\text{Ca}^{2+}$  levels and not signals caused by body movement. The  $\text{Ca}^{2+}$  signals increased rapidly from the attack onset and decayed slowly

after the tested mouse retreated to a safe area (Fig. 1E, F). Statistical analysis showed that the average value of the  $\text{Ca}^{2+}$  signals of BLA PNs increased significantly when a mouse was attacked by a CD-1 mouse (Fig. 1G), indicating that acute defeat stress strongly activates BLA PNs.

### CSDS Persistently Increases BLA Neuronal Activity

We then explored whether the changes in BLA activity were involved in the impairment of social behaviors induced by chronic stress. For this, we established a CSDS model. After 10 consecutive days of defeat stress, the SI test was used to divide the mice into SI-sus and SI-res groups (Fig. 2A). The SI ratio of the SI-sus mice was significantly lower than that of the control or SI-res mice (Fig. 2B, C). Furthermore, when compared to the control mice, the SI-sus mice spent less time in the interaction zone, while the SI-res mice spent more time in the interaction zone when the CD1 mouse was present in the mesh enclosure (Fig. 2D). On the other hand, the SI-sus but not the SI-res mice spent more time in the corner zone (Fig. 2E) suggesting that CSDS leads to social avoidance behavior in the former but not the latter.

We next assessed the dynamic changes of BLA activity at different stages of CSDS. The mice were allowed to freely explore in the presence or absence of a CD1 target in the mesh enclosure during the SI test. We recorded the peaks of  $\text{Ca}^{2+}$  signals that were time-locked with behavioral events (proximal interaction with the mesh enclosure) and then compared the amplitudes of these time-locked peaks across groups (Fig. 2F). Before CSDS, the  $\text{Ca}^{2+}$  signal peaks upon proximal interaction were comparable in the absence or presence of a CD1 mouse in both SI-sus and SI-res mice (Fig. 2G–I). One day after CSDS, the peaks were significantly increased in both groups when a CD1 mouse was present in the mesh enclosure (Fig. 2J, K), and the increased peaks triggered by a CD1 mouse did not differ between SI-sus and SI-res mice (Fig. 2L). To explore whether the increased  $\text{Ca}^{2+}$  peaks recovered differently upon cessation of the stress exposure, we then measured the BLA activity 20 days after CSDS. We found that the  $\text{Ca}^{2+}$  signal peaks upon proximal interaction were significantly increased in both groups when a CD1 mouse was in the mesh enclosure (Fig. 2M, N), indicating a lasting effect of CSDS. Notably, the increased peaks triggered by the CD1 mouse were much lower in the SI-res than the SI-sus mice (Fig. 2O). We then analyzed the correlation between BLA activity and social avoidance behavior as indicated by the SI ratio and found no significant correlation between the increased BLA activity and the SI ratio (Fig. 2P).

Taken together, these results indicate that CSDS increases social avoidance only in SI-sus mice and this

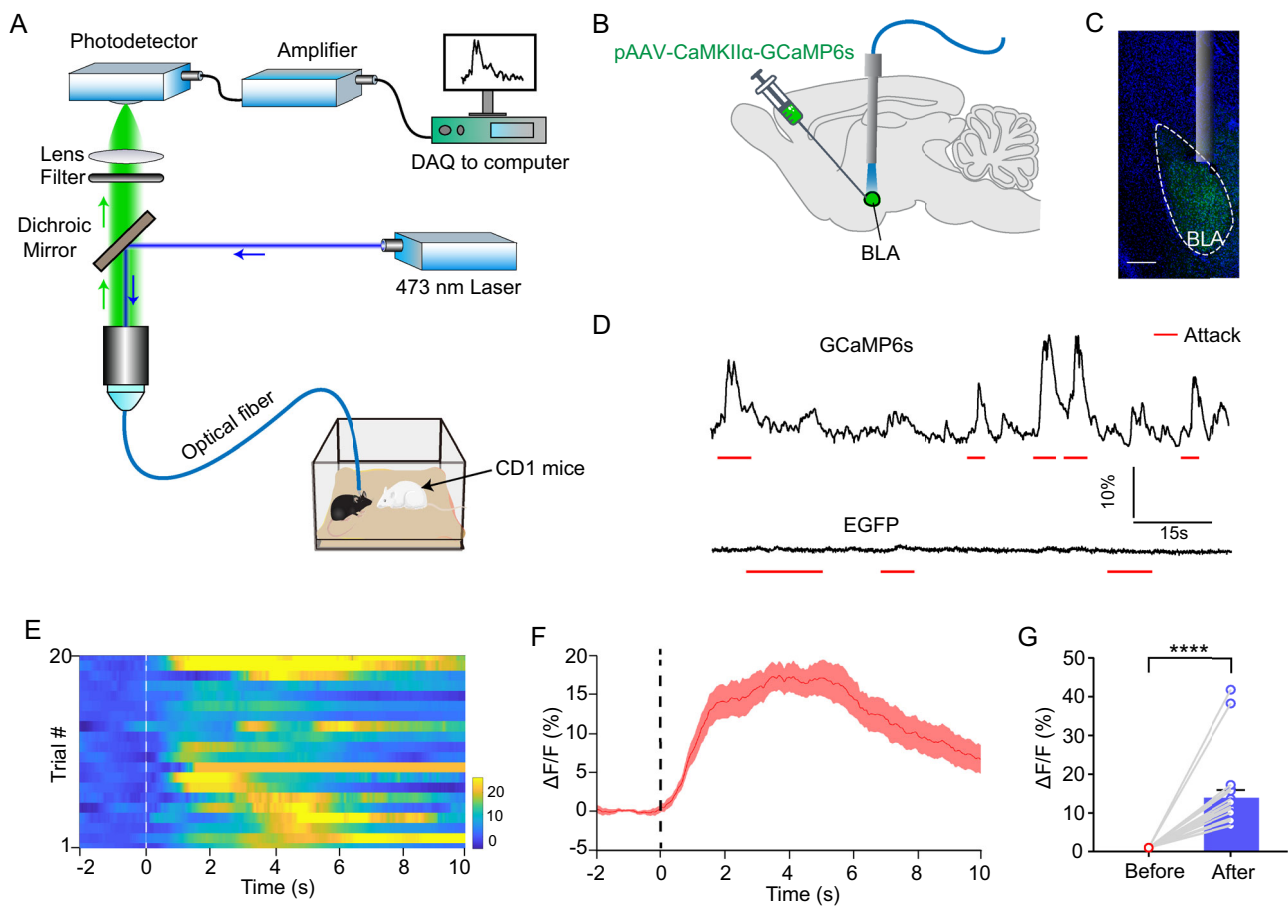


**Fig. 1** Acute defeat stress increases calcium signals in BLA projection neurons. **A** Schematic of the *in vivo* fiber photometry setup. **B** Diagram showing the injection of GCaMP6s-carrying adeno-associated virus (AAV) vectors into the BLA to record  $\text{Ca}^{2+}$  signals. **C** Representative image showing a cannula implanted onto the BLA (green, GCaMP6s expression in BLA neurons; blue, DAPI counterstaining of cell nuclei; scale bar, 200  $\mu\text{m}$ ). **D** Raw traces of fluorescence changes showing that social attack by a CD1 aggressor rapidly increases the  $\text{Ca}^{2+}$  signal in a GCaMP6s-expressing neuron (upper) but not in an EGFP-expressing neuron (lower) (red lines

indicate social attacks). **E** Trial-by-trial heatmap representation of  $\text{Ca}^{2+}$  signals in the BLA neurons from a GCaMP6s-expressing mouse. Each row represents a trial (20 trials from 8 mice). **F** Perievent plot of the averaged  $\text{Ca}^{2+}$  signals from the 8 mice as in (**E**). Thick line indicates the mean, and shaded area indicates the SEM. **G** Summary plots of the  $\Delta F/F$  signal before (2 s) and after attack (5 s) bouts in GCaMP6s-expressing BLA neurons ( $n = 20$ ;  $P < 0.0001$ , paired *t*-test; before attack: average  $\Delta F/F = 0\% \pm 0\%$ ; after attack: average  $\Delta F/F = 13.95\% \pm 2.06\%$ ; \*\*\*\* $P < 0.0001$ ).

increase does not appear to correlate with the enhanced BLA neuronal activity.

### CSDS Increases the Intrinsic Excitability of BLA Projection Neurons

To further reinforce the above finding that CSDS increased the BLA neuronal activity in both groups, we then used *ex vivo* slice electrophysiology to measure the excitability of BLA PN in acutely-prepared brain slices (Fig. 3A). We first injected depolarizing current pulses of increasing amplitude to induce APs. As shown in Figure 3B and C, the number of APs was significantly greater in the SI-sus and SI-res mice than in control mice; however, the input resistance did not differ among the three groups (Fig. 3D).

To support the above findings, we then measured the intrinsic excitability of BLA PN using another protocol by injecting a depolarizing current ramp into the cells. Similar results were found that the number of APs was significantly increased in both SI-sus and SI-res mice (Fig. 3E, F), while the rheobase (minimal current necessary to elicit an AP) remained unaltered (Fig. 3G). These results suggest that CSDS significantly increases the excitability of BLA neurons in both SI-sus and SI-res mice.

### CSDS Persistently Increases the Intrinsic Excitability of BLA Projection Neurons 20 Days After CSDS

To explore whether the increased intrinsic excitability of BLA PN persists after long-term recovery, we then



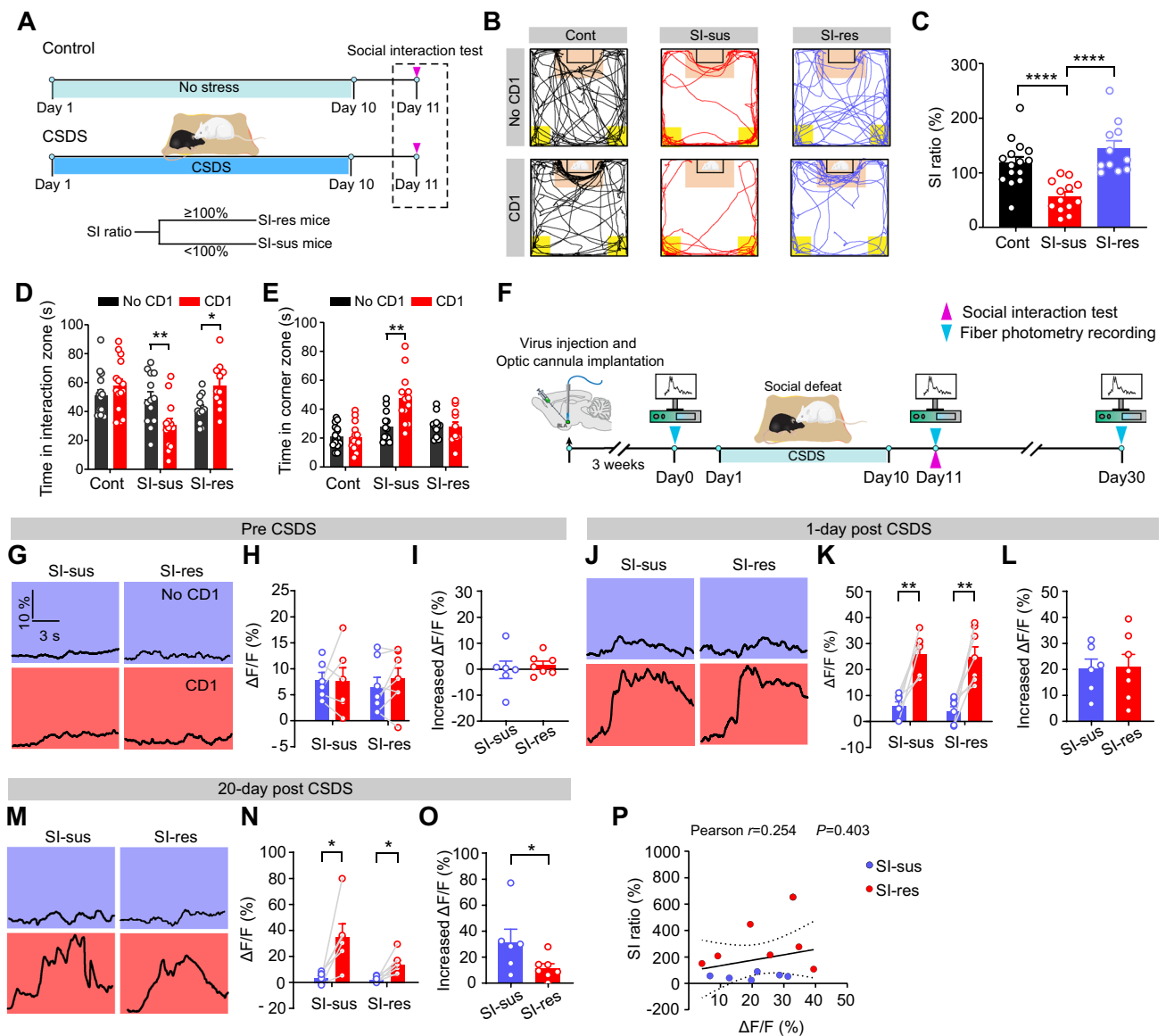


**Fig. 2** Chronic social defeat stress persistently activates BLA projection neurons. **A** Experimental procedures for controls and mice subjected to chronic social defeat stress (CSDS). **B** Representative activity tracking during the social interaction (SI) test for control, SI-sus, and SI-res mice in the absence or presence of a CD1 target. **C** Summary plots of the SI ratio of control (Cont), susceptible (SI-sus), and resilient (SI-res) mice (Cont,  $n = 15$  mice; SI-sus,  $n = 13$  mice; SI-res,  $n = 11$  mice; one-way ANOVA,  $F_{(2, 36)} = 15.97$ ,  $P < 0.0001$ ; Bonferroni *post hoc* comparison, Cont versus SI-sus,  $P = 0.0006$ ; Cont versus SI-res,  $P = 0.24$ ; SI-sus versus SI-res,  $P < 0.0001$ ). **D, E** Summary plots of time in interaction zone (**D**) and time in corner zone (**E**) of the three groups in the absence or presence of a CD1 target. Same sample sizes as in **C**. Time in interaction zone: two-way ANOVA, main effect of stress vulnerability:  $F_{(2, 36)} = 4.56$ ,  $P = 0.017$ ; main effect of CD1 present:  $F_{(1, 36)} = 0.29$ ,  $P = 0.59$ ; interaction:  $F_{(2, 36)} = 11.86$ ,  $P = 0.0001$ . Bonferroni *post hoc* comparison, SI-sus,  $P = 0.003$ ; SI-res,  $P = 0.014$ . Time in corner zone: two-way ANOVA, main effect of stress vulnerability:  $F_{(2, 36)} = 13.78$ ,  $P < 0.0001$ ; main effect of CD1 present:  $F_{(1, 36)} = 6.44$ ,  $P = 0.0157$ ; interaction:  $F_{(2, 36)} = 8.78$ ,  $P = 0.0008$ . Bonferroni *post hoc* comparison, SI-sus,  $P < 0.0001$ . **F** Experimental procedures for recording dynamic  $\text{Ca}^{2+}$  signals in BLA projection

neurons by *in vivo* fiber photometry. **G** Representative traces of  $\text{Ca}^{2+}$  signals aligned with first proximal interaction before CSDS in the absence (upper) or presence (lower) of a CD1 target. **H** Summary plots of  $\Delta F/F$  signal during proximal interaction before CSDS. The susceptible and resilient mice were defined after CSDS. SI-sus,  $n = 6$  mice; SI-res,  $n = 7$  mice.  $\Delta F/F$ : two-way ANOVA, main effect of CD1 present:  $F_{(1, 11)} = 0.18$ ,  $P = 0.679$ ; main effect of stress vulnerability:  $F_{(1, 11)} = 0.036$ ,  $P = 0.85$ ; interaction:  $F_{(1, 11)} = 0.297$ ,  $P = 0.597$ . **I** Percentage change in  $\Delta F/F$  signal in **H**. *t* test,  $P = 0.6$ . **J** Representative traces of  $\text{Ca}^{2+}$  signal 1-day after CSDS. **K** Summary plots as in **J**. Same sample sizes as in **H**.  $\Delta F/F$ : two-way ANOVA, main effect of CD1 present:  $F_{(1, 11)} = 43.29$ ,  $P < 0.0001$ ; main effect of stress vulnerability:  $F_{(1, 11)} = 0.367$ ,  $P = 0.557$ ; interaction:  $F_{(1, 11)} = 0.017$ ,  $P = 0.9$ . **L** Percentage change in  $\Delta F/F$  in **J**. *t* test,  $P = 0.9$ . **M** Representative traces of  $\text{Ca}^{2+}$  signal 20 days after CSDS. **N** Summary plots as in **M**. Same sample sizes as in **H**.  $\Delta F/F$ : Wilcoxon signed-rank test. SI-sus,  $P = 0.028$ ; SI-res,  $P = 0.018$ . **O** Percentage change in  $\Delta F/F$  as in **L**. Mann-Whitney test,  $P = 0.035$ . **P** Correlation between the SI ratio and  $\Delta F/F$  in stressed mice. Pearson  $r = 0.254$ ,  $P = 0.403$ . All data are presented as the mean  $\pm$  SEM. \* $P < 0.05$ , \*\* $P < 0.01$ , \*\*\*\* $P < 0.0001$ .

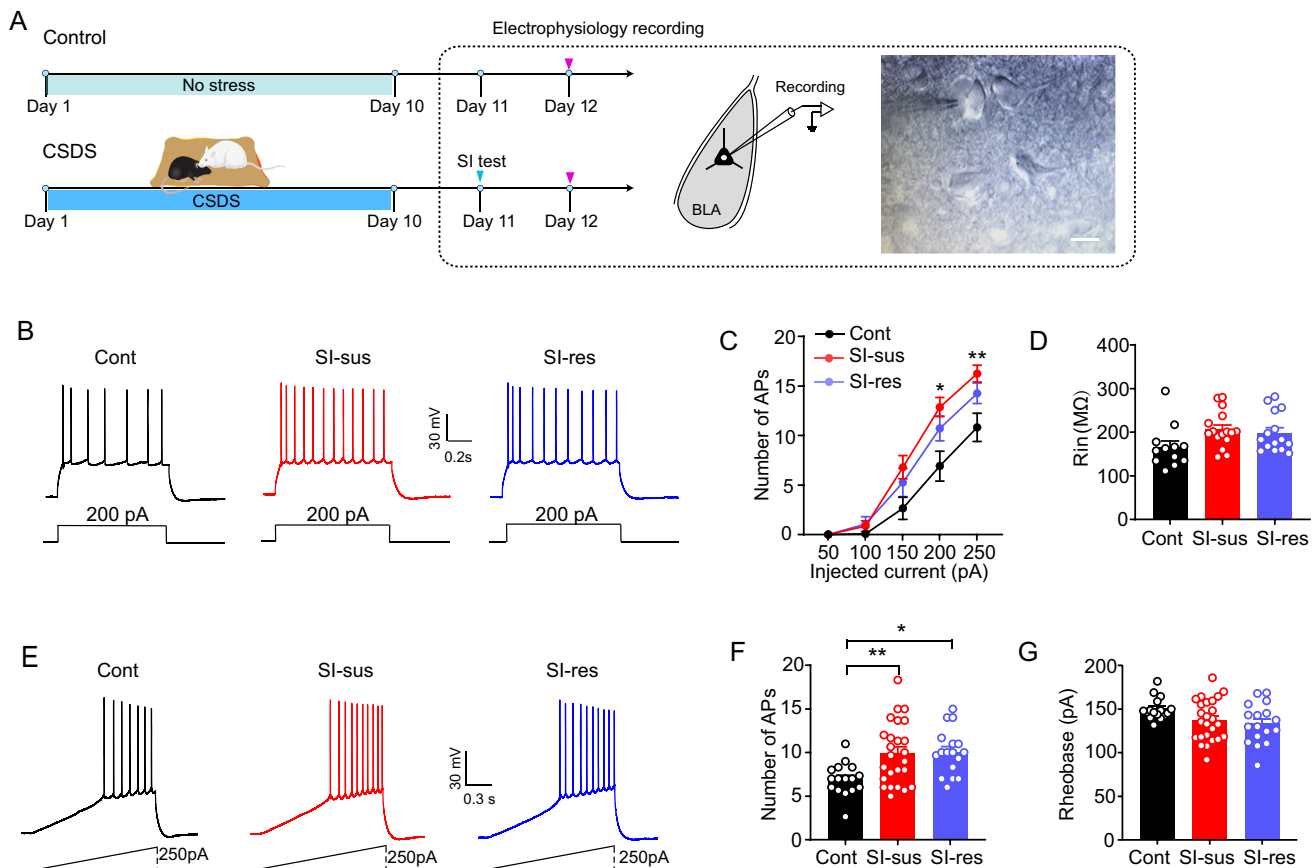


**Fig. 3** CSDS increases the intrinsic excitability of BLA projection neurons. **A** Experimental procedures for electrophysiological recordings in controls and mice subjected to chronic social defeat stress (CSDS) (scale bar, 15  $\mu$ m). **B** Representative traces of action potential (AP) firing in response to injection of current from control (Cont), susceptible (SI-sus), and resilient (SI-res) mice (scale bars, 0.2 s, 30 mV). **C** Summary plots of AP numbers as a function of injected current strength, as in (**B**). Cont,  $n = 12$  neurons/3 mice; SI-sus,  $n = 16$  neurons/5 mice; SI-res,  $n = 15$  neurons/4 mice. two-way ANOVA, main effect of depolarization steps:  $F_{(4, 160)} = 252.3$ ,  $P < 0.0001$ ; main effect of CSDS:  $F_{(2, 40)} = 4.463$ ,  $P = 0.0178$ ; main effect of interaction:  $F_{(8, 160)} = 4.223$ ,  $P = 0.0001$ . Bonferroni *post hoc*

comparison, current strength = 200 pA, Cont vs SI-sus,  $P < 0.0001$ , Cont vs SI-res,  $P = 0.021$ ; current strength = 250 pA, Cont vs SI-sus,  $P = 0.0004$ , Cont vs SI-res,  $P = 0.046$ . **D** Summary plots of input resistance ( $R_{in}$ ). One-way ANOVA,  $F_{(2,40)} = 2.953$ ,  $P = 0.0636$ . **E** As in (**B**), except that ramped depolarizing current is injected into BLA projection neurons. **F** Summary plots of AP numbers, as in (**E**). Cont,  $n = 16$  neurons/4 mice; SI-sus,  $n = 25$  neurons/6 mice; SI-res,  $n = 17$  neurons/5 mice. One-way ANOVA,  $F_{(2,55)} = 6.318$ ,  $P = 0.0034$ . Bonferroni *post hoc* comparison, Cont vs SI-sus,  $P = 0.0065$ ; Cont vs SI-res,  $P = 0.0104$ . **G** Summary plots of rheobase of APs, as in (**E**). One-way ANOVA,  $F_{(2,55)} = 3.032$ ,  $P = 0.0564$ . All data are presented as the mean  $\pm$  SEM. \* $P < 0.05$ , \*\* $P < 0.01$ .

recorded their firing in all three groups of mice 20 days after CSDS (Fig. 4A). Similarly, the results showed that the number of APs induced by depolarizing current injection was significantly increased in the SI-sus and SI-res mice (Fig. 4B, C), while the input resistance did not differ among the three groups (Fig. 4D). In parallel, the results of injection of a ramp of depolarizing current also showed that the number of APs, but not the rheobase, was increased in both SI-sus and SI-res mice (Fig. 4E–G). These results argue that CSDS persistently increases the intrinsic excitability of BLA PNs in both SI-sus and SI-res mice.

### CSDS Persistently Induces Anxiety-Like Behavior in SI-sus and SI-res Mice

The above results indicated that CSDS results in a persistent increase of BLA neuronal activity in both SI-sus and SI-res mice, suggesting that this activity may not be responsible for CSDS-induced social avoidance behavior. A large number of studies have consistently shown that the increased activity of amygdala neurons is strongly associated with stress-related anxiety-like behaviors [20, 30]. We then measured the anxiety-like behaviors in SI-sus and SI-res mice 1 day after CSDS using the OFT and EPM (Fig. 5A). Relative to the control mice, both the SI-sus and SI-res mice spent less time in the center area of the open field chamber during the OFT (Fig. 5B, C), while no

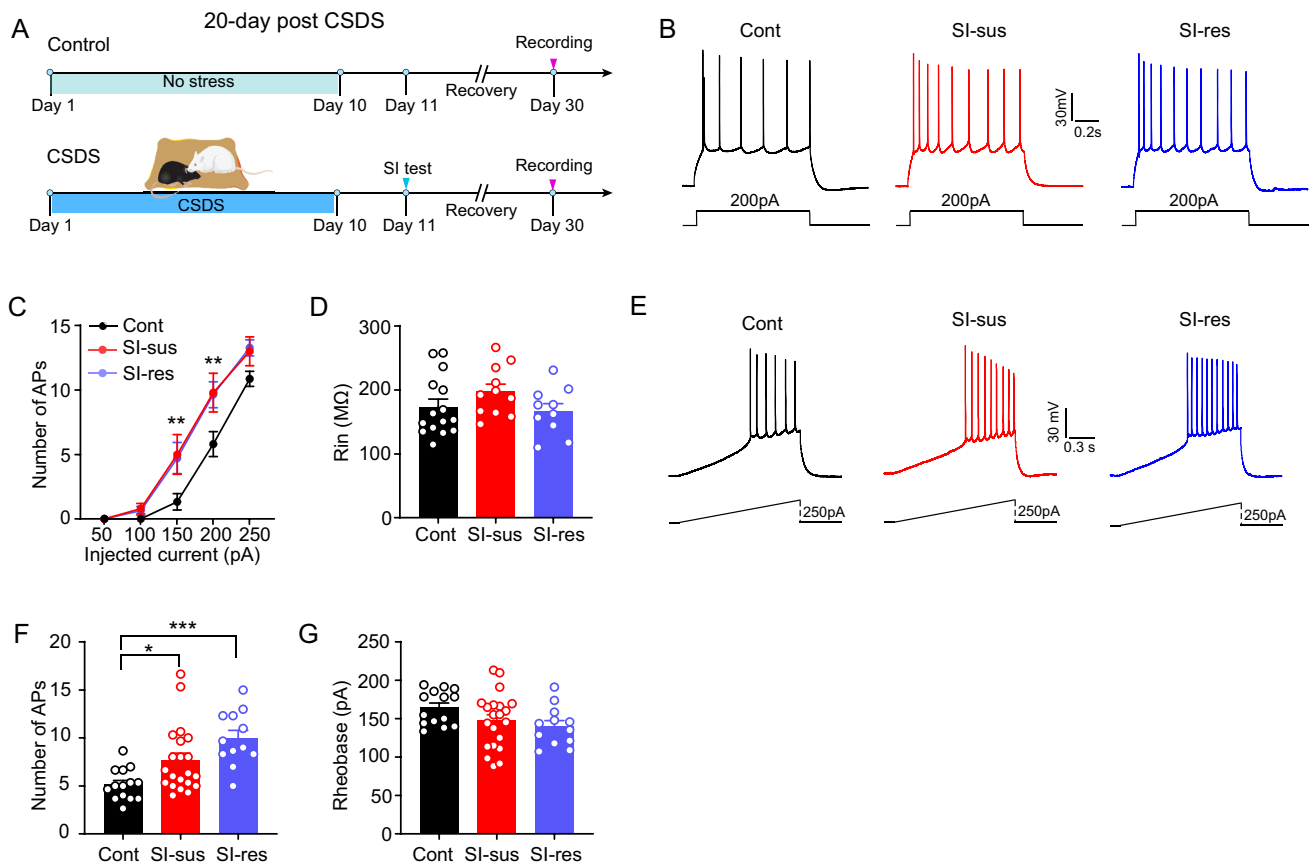


**Fig. 4** The augmented excitability of BLA projection neurons persists 20 days after CSDS. **A** Experimental procedures for electrophysiological recordings. **B** Representative traces of action potential (AP) firing in response to injection of current from control (Cont), susceptible (SI-sus), and resilient (SI-res) mice. **C** Summary plots of AP numbers as a function of injected current, as in (**B**). Cont,  $n = 15$  neurons/5 mice; SI-sus,  $n = 11$  neurons/3 mice; SI-res,  $n = 10$  neurons/3 mice. Two-way ANOVA, main effect of depolarizing steps:  $F_{(4, 132)} = 261.4$ ,  $P < 0.0001$ ; main effect of CSDS:  $F_{(2, 33)} = 4.361$ ,  $P = 0.0209$ ; main effect of interaction:  $F_{(8, 132)} = 3.406$ ,  $P = 0.0014$ . Bonferroni *post hoc* comparison, current strength = 150 pA, Cont vs SI-sus,  $P = 0.004$ , Cont vs SI-res,  $P = 0.006$ ; current strength

= 200 pA, Cont vs SI-sus,  $P = 0.001$ , Cont vs SI-res,  $P = 0.002$ . **D** Summary plots of Rin. One-way ANOVA,  $F_{(2,33)} = 1.621$ ,  $P = 0.213$ . **E** As in (**B**), except that ramped depolarizing current is injected into BLA projection neurons. **F** Summary plots of AP numbers, as in (**E**). Cont,  $n = 14$  neurons/5 mice; SI-sus,  $n = 21$  neurons/6 mice; SI-res,  $n = 12$  neurons/3 mice. One-way ANOVA,  $F_{(2,44)} = 9.276$ ,  $P = 0.0004$ . Bonferroni *post hoc* comparison, Cont vs SI-sus,  $P = 0.0422$ ; Cont vs SI-res,  $P = 0.0003$ . **G** Summary plots of rheobase of APs, as in (**E**). One-way ANOVA,  $F_{(2,44)} = 2.367$ ,  $P = 0.0106$ . Bonferroni *post hoc* comparison, Cont vs SI-sus,  $P = 0.3129$ ; Cont vs SI-res,  $P = 0.133$ . All data are presented as the mean  $\pm$  SEM. \* $P < 0.05$ , \*\* $P < 0.01$ , \*\*\* $P < 0.001$ .

significant differences were found in the total distance traveled (Fig. 5D). Besides, the EPM results showed that the SI-sus and SI-res mice spent less time in the open arms (Fig. 5E, F) and had fewer entries into these arms (Fig. 5G). To explore whether CSDS has a long-lasting influence, we also tested the anxiety-like behavior after 20 days of recovery from CSDS (Fig. 6A). Both SI-sus and SI-res mice spent less time in the center area (Fig. 6B, C), while the total distance traveled remained unaltered during the OFT (Fig. 6D). The EPM results also showed that the SI-sus and SI-res mice spent less time in the open arms (Fig. 6E, F) and had fewer entries to these arms (Fig. 6G) EPM. Together, these results indicate that CSDS persistently increases the anxiety-like behavior of mice regardless of their susceptible or resilient nature.

### CSDS-Induced Increase of BLA Neuronal Excitability is Correlated with Anxiety-Like, but not Social Avoidance Behavior

Stress-induced anxiety has long been linked to the hyperactivation of amygdala neurons [20]. We then asked whether there is a relationship between BLA neuronal activity and anxiety-like behavior. To this end, we first measured the anxiety-like behavior using the OFT and EPM. Four hours later, the neuronal activity was evaluated by the number of APs in response to step or ramp depolarizing current injection. The AP numbers (averaged from 3–5 cells per mouse) were significantly and inversely correlated with all the parameters of anxiety-like behavior, including time spent in the center of the OFT and time



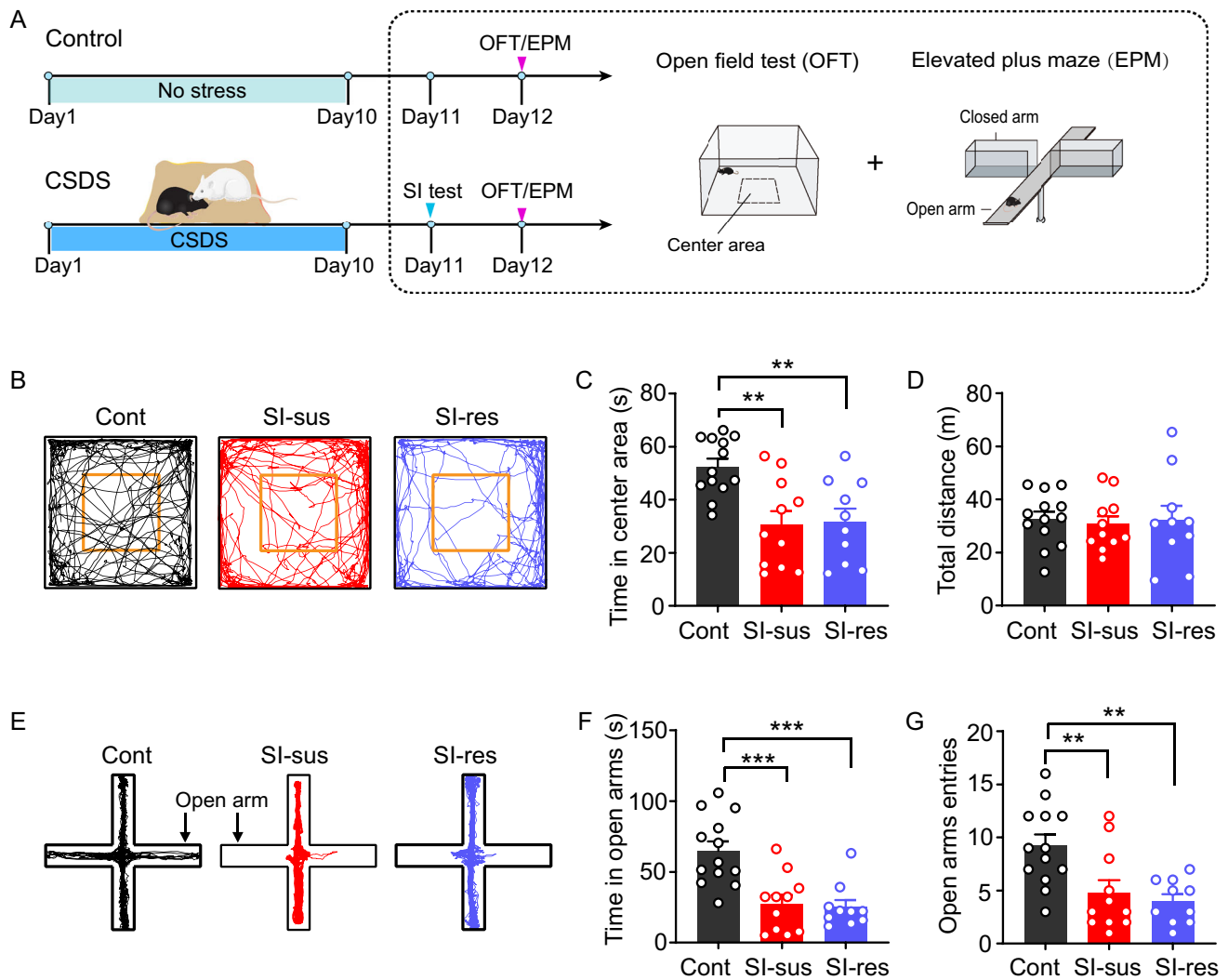


**Fig. 5** CSDS increases anxiety-like behavior in SI-sus and SI-res mice. **A** Experimental procedures for anxiety-like behavioral tests. **B** Representative activity tracking in the OFT for control (Cont), susceptible (SI-sus), and resilient (SI-res) mice. **C** Summary plots of time in center area in the OFT. Cont,  $n = 13$  mice; SI-sus,  $n = 11$  mice; SI-res,  $n = 10$  mice. One-way ANOVA,  $F_{(2,31)} = 8.985$ ,  $P = 0.0008$ . Bonferroni *post hoc* comparison, Cont vs SI-sus,  $P = 0.0022$ ; Cont vs SI-res,  $P = 0.0044$ . **D** Summary plots of total distance travelled in the OFT. One-way ANOVA,  $F_{(2,31)} = 0.079$ ,  $P = 0.924$ .

spent in open arms of the EPM apparatus (Fig. 7A–D). However, no significant correlations were found between AP number and the SI ratio (Fig. 7E, F). Furthermore, there were no correlations between anxiety-like behaviors and the SI ratio (Fig. 7G, H). These data therefore support a link between the increased BLA neuronal activity and CSDS-related increases in anxiety-like behavior rather than social avoidance behavior.

**E** Representative activity tracking in the EPM. **F** Summary plots of time in open arms. Same sample sizes as in C. One-way ANOVA,  $F_{(2,31)} = 13.74$ ,  $P < 0.0001$ . Bonferroni *post hoc* comparison, Cont vs SI-sus,  $P = 0.0004$ ; Cont vs SI-res,  $P = 0.0002$ . **G** Summary plots of open arms entries. Same sample sizes as in C. One-way ANOVA,  $F_{(2,31)} = 8.262$ ,  $P = 0.0013$ . Bonferroni *post hoc* comparison, Cont vs SI-sus,  $P = 0.0089$ ; Cont vs SI-res,  $P = 0.0025$ . All data are presented as the mean  $\pm$  SEM. \*\* $P < 0.01$ , \*\*\* $P < 0.001$ .

## Discussion

In the present study, using *in vivo* fiber photometry and *in vitro* electrophysiology, we found that CSDS persistently increased BLA neuronal activity in both SI-sus and SI-res mice. This increase correlated well with the concomitant increase of anxiety-like behavior, as found in both groups. By contrast, it did not correlate with heightened social avoidance behavior, which was only evident in the SI-res mice.

Considerable evidence has indicated that aberrant neuronal activity and hyperexcitability in the BLA are

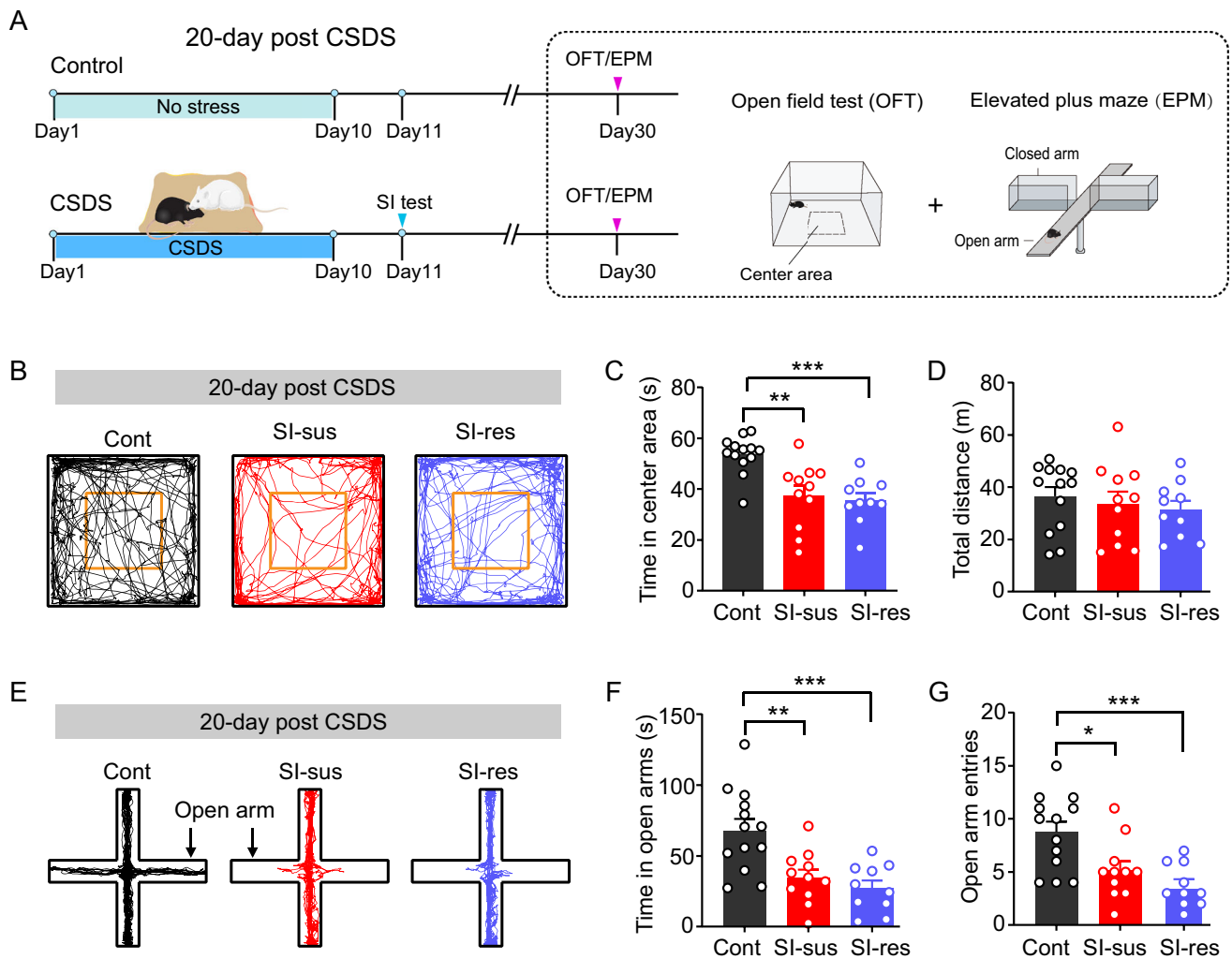


**Fig. 6** CSDS persistently increases anxiety-like behavior in SI-sus and SI-res mice 20 days after CSDS. **A** Experimental procedures for anxiety-like behavioral tests 20-day after CSDS. **B** Representative activity tracking in the OFT for control (Cont), susceptible (SI-sus), and resilient (SI-res) mice. **C** Summary plots of time in center area in the OFT. Cont,  $n = 13$  mice; SI-sus,  $n = 11$  mice; SI-res,  $n = 10$  mice. One-way ANOVA,  $F_{(2,31)} = 15.85$ ,  $P < 0.0001$ . Bonferroni *post hoc* comparison, Cont vs SI-sus,  $P < 0.0001$ ; Cont vs SI-res,  $P = 0.0002$ . **D** Summary plots of total distance travelled in the OFT. One-way

ANOVA,  $F_{(2,31)} = 0.443$ ,  $P = 0.646$ . **E** Representative activity tracking in the EPM for the three groups. **F** Summary plots of time in open arms in the EPM. Same sample size as in **C**. One-way ANOVA,  $F_{(2,31)} = 12.81$ ,  $P < 0.0001$ . Bonferroni *post hoc* comparison, Cont vs SI-sus,  $P = 0.0007$ ; Cont vs SI-res,  $P = 0.0003$ . **G** Summary plots of open arm entries in the EPM. One-way ANOVA,  $F_{(2,31)} = 9.292$ ,  $P = 0.0007$ . Bonferroni *post hoc* comparison, Cont vs SI-sus,  $P = 0.0146$ ; Cont vs SI-res,  $P = 0.0008$ . All data are presented as the mean  $\pm$  SEM. \*  $P < 0.05$ , \*\*  $P < 0.01$ , \*\*\*  $P < 0.001$ .

involved in the occurrence of multiple stress-related psychiatric disorders, such as social disorder [3] and anxiety disorder [18]. Our findings that acute social attack significantly increased the BLA neuronal activity are consistent with a recent finding showing that BLA activity is dramatically increased during acute restraint stress, also assessed by *in vivo* fiber photometry [32]. However, the long-term effect of chronic stress on BLA neuronal activity was not yet known. Here, we found that the increased BLA neuronal activity persisted 1 day and even 20 days after exposure to chronic stress. To our knowledge, this is the first study to measure the long-term changes of BLA neuronal activity in response to chronic stress in freely-

moving mice. Somewhat surprisingly, our results showed that the increased BLA activity existed in both SI-sus and SI-res mice [5, 33]. Confirming this, the *ex vivo* patch-clamp results also showed that CSDS increased the intrinsic excitability in both groups, suggesting that stress susceptibility defined by social avoidance behavior may not be associated with BLA activity. In parallel, a study using magnetic resonance imaging in CSDS mice revealed that the amygdala volume is comparable in susceptible and resilient mice [34].

Notably, similar to the increased BLA neuronal activity in both SI-sus and SI-res mice, we found that the anxiety-like behavior was also increased by CSDS in both. This is

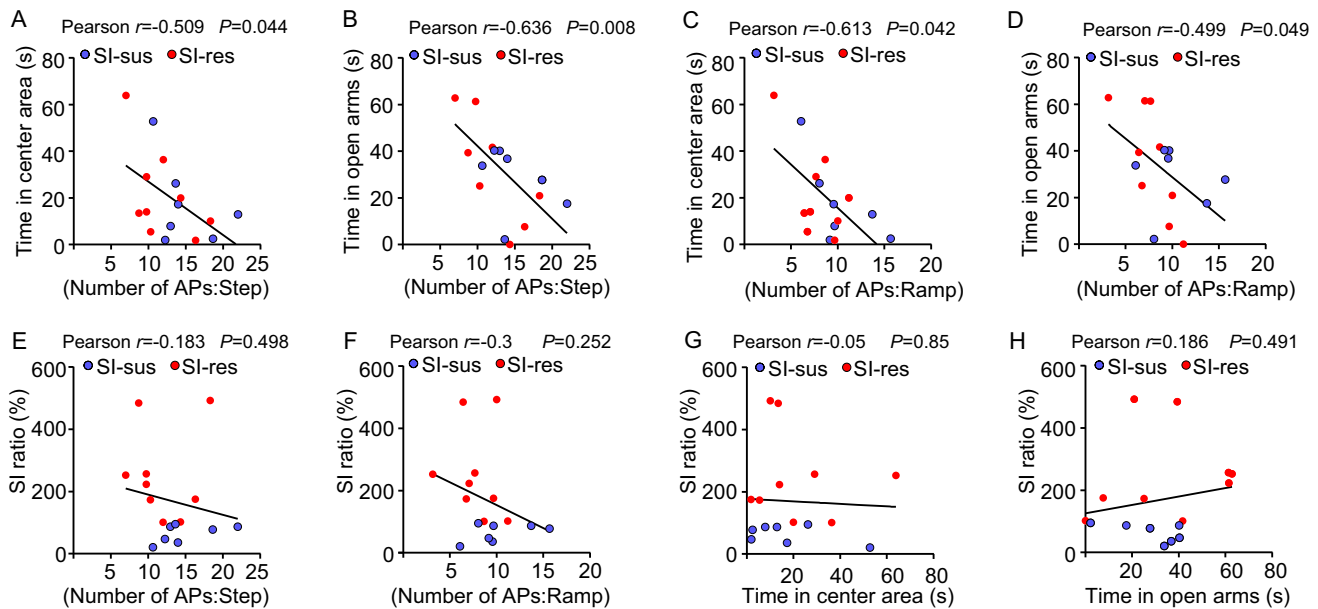


**Fig. 7** Correlations between CSDS-induced increase of BLA neuronal activity and anxiety-like behavior and social avoidance behavior. **A, B** Correlations between the AP numbers induced by step current injection and time in center region in the OFT (**A**) and time in open arms in the EPM (**B**) (AP number in response to injection current of 250 pA). **C, D** Correlations between the AP numbers induced by ramp current injection and time in center region

in the OFT (**C**) and time in open arms in the EPM (**D**). **E, F** Correlations between SI ratio and the AP numbers induced by step (**E**) and ramp (**F**) depolarizing current injection. **G, H** Correlations between SI ratio and time in center region in the OFT (**G**) and time in open arms in the EPM (**H**).  $n = 16$  mice. Note that two data sets are overlapped in **B**.

in good accordance with a previous study showing that CSDS causes a prolonged increase of anxiety-like behavior in both SI-sus and SI-res mice even after long-lasting stress-free recovery [5]. Numerous studies have shown that stress-induced anxiety-like behavior results from the hyperactivation of BLA neurons [20, 28, 29], and these findings further suggest that the CSDS-induced, persistent increase of BLA activity contributes to excessive anxiety-like behavior in mice, regardless of their susceptible or resilient nature. Since only the SI-sus, but not the SI-res mice exhibit depressive-like behaviors, CSDS has been widely used to explore the mechanism of vulnerability to depression [5]. However, the findings from our and others' studies imply that the SI ratio may not be appropriate to differentiate the susceptibility to stress-induced anxiety in mice [5]. In addition to CSDS, several other stress models, including learned helplessness [35], chronic mild stress [36], and exposure to predator odor [37], have also been used to classify animals into susceptible and resilient subsets based on their performance in specific behavioral tasks. For example, a previous study defined susceptibility by the adrenal gland weight of mice subjected to repeated restraint stress [38]. There are also studies using the light-dark behavioral test, another widely-used paradigm for measuring anxiety-like behavior, to define stress susceptibility (high level of anxiety-like behavior) and resilience (low level of anxiety-like behavior) [39, 40]. Using

multiple models and behavioral paradigms may help to precisely identify the individual differences in stress vulnerability and explore the underlying neuronal mechanisms.

Mounting evidence has demonstrated that many of the psychiatric symptoms and biological changes persist even long after recovery from chronic stress or traumatic events [41–43]. For example, mice display robust social avoidance behavior four weeks after CSDS [41, 44]. Similarly, it has been reported that four weeks after CSDS, the social avoidance behavior of susceptible mice is still increased, and susceptible and resilient mice still have high anxiety levels [5]. These findings are consistent with our results that mice remained at a high anxiety level even after 20 days of recovery. In addition, a recent study has shown that CSDS increases the dendritic arborization of BLA stellate neurons after 30 days of stress-free recovery, accompanied by remarkable social avoidance behavior when exposed to a fearful stimulus [43]. In line with this, the activity and intrinsic excitability of BLA neurons were also persistently increased, arguing for a critical role of BLA activity in stress-induced anxiety-like behavior. Interestingly, our fiber photometry results showed that the BLA activity was significantly decreased in SI-res mice 20 days after CSDS, suggesting that SI-res mice are more adaptable than their SI-sus counterparts.

The increase of BLA activity by chronic stress may facilitate the transmission of information from the BLA to its downstream regions, such as the medial prefrontal cortex (mPFC) and ventral hippocampus (vHPC) [16]. Circuit-specific manipulations have revealed that activation of BLA neuronal subpopulations projecting to different downstream regions are responsible for different or even opposite behaviors. For instance, optogenetic activation of BLA PNs projecting to the mPFC or vHPC leads to anxiety-like behavior. In contrast, activation of BLA PNs that project to the anterodorsal bed nucleus of the stria terminalis and central lateral amygdala results in an anxiolytic effect [45, 46]. Consistent with this, our recent study has shown that chronic stress-induced anxiety-like behavior is associated with the selective enhancement of the activity of BLA PNs that project to the vHPC [30]. Notably, studies have shown that activation of the BLA–mPFC or BLA–vHPC circuit also leads to social avoidance behavior [47, 48]. Although we did not find any correlation between social avoidance behavior and the activity of BLA PNs as a whole, we cannot exclude the possibility that the stress-related social avoidance behavior may engage specific BLA circuits. Indeed, increasing evidence has highlighted a circuit-specific mechanism in stress resilience. For instance, activation of the ventral tegmental area (VTA)–nucleus accumbens (NAc), but not the VTA–mPFC circuit results in stress susceptibility [49]. Strikingly, activity of vHPC neurons is decreased in resilient mice, while vHPC–NAc synaptic transmission is selectively increased in susceptible mice [50]. Besides, studies have also emerged to link increased amygdala activity and amygdala–prefrontal connectivity to resilience to early life stress [51]. Therefore, it would be rather interesting to delineate the dynamic changes of neuronal activity of specific BLA circuits in susceptible and resilient mice.

In summary, the current findings indicate that increased BLA neuronal activity may not contribute to the pathological process of social disorder. Instead, it may play essential roles in stress-induced anxiety-like behavior. These findings provide new insight into the role of neuronal activity in the amygdala in mediating stress-related psychiatric disorders.

**Acknowledgements** This work was supported by grants from the National Natural Science Foundation of China (31970953, 81930032, and 81760505) and the Natural Science Foundation of Jiangxi Province, China (20192ACB21024, 20192ACB20023, 20181ACG70003, and 20192BCB23008).

**Conflict of interest** The authors declare that no competing interests.

## References

- de Kloet ER, Joëls M, Holsboer F. Stress and the brain: From adaptation to disease. *Nat Rev Neurosci* 2005, 6: 463–475.
- Craske MG, Stein MB, Eley TC, Milad MR, Holmes A, Rapee RM. Anxiety disorders. *Nat Rev Dis Primers* 2017, 3: 1–19.
- Twining RC, Vantrease JE, Love S, Padival M, Rosenkranz JA. An intra-amygdala circuit specifically regulates social fear learning. *Nat Neurosci* 2017, 20: 459–469.
- Yin YN, Hu J, Wei YL, Li ZL, Luo ZC, Wang RQ, *et al.* Astrocyte-derived lactate modulates the passive coping response to behavioral challenge in male mice. *Neurosci Bull* 2021, 37: 1–14.
- Krishnan V, Han MH, Graham DL, Berton O, Renthal W, Russo SJ, *et al.* Molecular adaptations underlying susceptibility and resistance to social defeat in brain reward regions. *Cell* 2007, 131: 391–404.
- Russo SJ, Murrrough JW, Han MH, Charney DS, Nestler EJ. Neurobiology of resilience. *Nat Neurosci* 2012, 15: 1475–1484.
- Bagot RC, Cates HM, Purushothaman I, Lorsch ZS, Walker DM, Wang J, *et al.* Circuit-wide transcriptional profiling reveals brain region-specific gene networks regulating depression susceptibility. *Neuron* 2016, 90: 969–983.
- Han MH, Nestler EJ. Neural substrates of depression and resilience. *Neurotherapeutics* 2017, 14: 677–686.
- Burke AR, McCormick CM, Pellis SM, Lukkes JL. Impact of adolescent social experiences on behavior and neural circuits implicated in mental illnesses. *Neurosci Biobehav Rev* 2017, 76: 280–300.
- Li MX, Zheng HL, Luo Y, He JG, Wang W, Han J, *et al.* Gene deficiency and pharmacological inhibition of caspase-1 confers resilience to chronic social defeat stress via regulating the stability of surface AMPARs. *Mol Psychiatry* 2018, 23: 556–568.
- Shen CJ, Zheng D, Li KX, Yang JM, Pan HQ, Yu XD, *et al.* Cannabinoid CB<sub>1</sub> receptors in the amygdalar cholecystokinin glutamatergic afferents to nucleus accumbens modulate depressive-like behavior. *Nat Med* 2019, 25: 337–349.
- Pfau ML, Russo SJ. Peripheral and central mechanisms of stress resilience. *Neurobiol Stress* 2015, 1: 66–79.
- Espallergues J, Teegarden SL, Veerakumar A, Boulden J, Challis C, Jochems J, *et al.* HDAC6 regulates glucocorticoid receptor signaling in serotonin pathways with critical impact on stress resilience. *J Neurosci* 2012, 32: 4400–4416.
- Donahue RJ, Muschamp JW, Russo SJ, Nestler EJ, Carlezon WA Jr. Effects of striatal  $\Delta$ FosB overexpression and ketamine on social defeat stress-induced anhedonia in mice. *Biol Psychiatry* 2014, 76: 550–558.
- Sah P, Faber ES, Lopez De Armentia M, Power J. The amygdaloid complex: Anatomy and physiology. *Physiol Rev* 2003, 83: 803–834.
- Janak PH, Tye KM. From circuits to behaviour in the amygdala. *Nature* 2015, 517: 284–292.
- Fu JY, Yu XD, Zhu Y, Xie SZ, Tang MY, Yu B, *et al.* Whole-brain map of long-range monosynaptic inputs to different cell types in the amygdala of the mouse. *Neurosci Bull* 2020, 36: 1381–1394.
- Padival M, Quinette D, Rosenkranz JA. Effects of repeated stress on excitatory drive of basal amygdala neurons *in vivo*. *Neuropsychopharmacology* 2013, 38: 1748–1762.
- LeDoux J. The amygdala. *Curr Biol* 2007, 17: R868–R874.
- Rosenkranz JA, Venheim ER, Padival M. Chronic stress causes amygdala hyperexcitability in rodents. *Biol Psychiatry* 2010, 67: 1128–1136.
- Liu ZP, Song C, Wang M, He Y, Xu XB, Pan HQ, *et al.* Chronic stress impairs GABAergic control of amygdala through

- suppressing the tonic GABAA receptor currents. *Mol Brain* 2014, 7: 32.
22. Liu ZP, He QH, Pan HQ, Xu XB, Chen WB, He Y, *et al.* Delta subunit-containing gamma-aminobutyric acid A receptor disinhibits lateral amygdala and facilitates fear expression in mice. *Biol Psychiatry* 2017, 81: 990–1002.
  23. Zhang WH, Zhang JY, Holmes A, Pan BX. Amygdala circuit substrates for stress adaptation and adversity. *Biol Psychiatry* 2021, 89: 847–856.
  24. Gunaydin LA, Grosenick L, Finkelstein JC, Kauvar IV, Fenno LE, Adhikari A, *et al.* Natural neural projection dynamics underlying social behavior. *Cell* 2014, 157: 1535–1551.
  25. Calipari ES, Bagot RC, Purushothaman I, Davidson TJ, Yorgason JT, Peña CJ, *et al.* *In vivo* imaging identifies temporal signature of D1 and D2 medium spiny neurons in cocaine reward. *PNAS* 2016, 113: 2726–2731.
  26. Wang DQ, Li Y, Feng QR, Guo QC, Luo MM. Learning shapes the aversion and reward responses of lateral habenula neurons. *Elife Sci* 2017, 6: e23045.
  27. Li Y, Liu Z, Guo Q, Luo M. Long-term fiber photometry for neuroscience studies. *Neurosci Bull* 2019, 35: 425–433.
  28. Qin X, He Y, Wang N, Zou JX, Zhang YM, Cao JL, *et al.* Moderate maternal separation mitigates the altered synaptic transmission and neuronal activation in amygdala by chronic stress in adult mice. *Mol Brain* 2019, 12: 111.
  29. Pan HQ, Zhang WH, Liao CZ, He Y, Xiao ZM, Qin X, *et al.* Chronic stress oppositely regulates tonic inhibition in Thy1-expressing and non-expressing neurons in amygdala. *Front Neurosci* 2020, 14: 299.
  30. Zhang WH, Liu WZ, He Y, You WJ, Zhang JY, Xu H, *et al.* Chronic stress causes projection-specific adaptation of amygdala neurons via small-conductance calcium-activated potassium channel downregulation. *Biol Psychiatry* 2019, 85: 812–828.
  31. Zheng ZH, Tu JL, Li XH, Hua Q, Liu WZ, Liu Y, *et al.* Neuroinflammation induces anxiety- and depressive-like behavior by modulating neuronal plasticity in the basolateral amygdala. *Brain Behav Immun* 2021, 91: 505–518.
  32. Morgan A, Gaudlen A, Altemus M, Williford K, Centanni S, Winder D, *et al.* Cyclooxygenase-2 inhibition prevents stress induced amygdala activation and anxiety-like behavior. *Brain Behav Immun* 2020, 89: 513–517.
  33. Golden SA, Covington HE, Berton O, Russo SJ. A standardized protocol for repeated social defeat stress in mice. *Nat Protoc* 2011, 6: 1183–1191.
  34. Anacker C, Scholz J, O'Donnell KJ, Allemang-Grand R, Diorio J, Bagot RC, *et al.* Neuroanatomic differences associated with stress susceptibility and resilience. *Biol Psychiatry* 2016, 79: 840–849.
  35. Berton O, Covington HE, Ebner K, Tsankova NM, Carle TL, Ulery P, *et al.* Induction of  $\Delta$ FosB in the periaqueductal gray by stress promotes active coping responses. *Neuron* 2007, 56: 574.
  36. Delgado y Palacios R, Campo A, Henningsen K, Verhoye M, Poot D, Dijkstra J, *et al.* Magnetic resonance imaging and spectroscopy reveal differential hippocampal changes in anhedonic and resilient subtypes of the chronic mild stress rat model. *Biol Psychiatry* 2011, 70: 449–457.
  37. Cohen H, Liu TM, Kozlovsky N, Kaplan Z, Zohar J, Mathé AA. The neuropeptide Y (NPY)-ergic system is associated with behavioral resilience to stress exposure in an animal model of post-traumatic stress disorder. *Neuropsychopharmacology* 2012, 37: 350–363.
  38. Hetzel A, Rosenkranz JA. Distinct effects of repeated restraint stress on basolateral amygdala neuronal membrane properties in resilient adolescent and adult rats. *Neuropsychopharmacology* 2014, 39: 2114–2130.
  39. Nasca C, Bigio B, Zelli D, Nicoletti F, McEwen BS. Mind the gap: Glucocorticoids modulate hippocampal glutamate tone underlying individual differences in stress susceptibility. *Mol Psychiatry* 2015, 20: 755–763.
  40. Nasca C, Menard C, Hodes G, Bigio B, Pena C, Lorsch Z, *et al.* Multidimensional predictors of susceptibility and resilience to social defeat stress. *Biol Psychiatry* 2019, 86: 483–491.
  41. Berton O, McClung CA, Dileone RJ, Krishnan V, Renthal W, Russo SJ, *et al.* Essential role of BDNF in the mesolimbic dopamine pathway in social defeat stress. *Science* 2006, 311: 864–868.
  42. Lagace DC, Donovan MH, DeCarolis NA, Farnbauch LA, Malhotra S, Berton O, *et al.* Adult hippocampal neurogenesis is functionally important for stress-induced social avoidance. *PNAS* 2010, 107: 4436–4441.
  43. Colyn L, Venzala E, Marco S, Perez-Otaño I, Tordera RM. Chronic social defeat stress induces sustained synaptic structural changes in the prefrontal cortex and amygdala. *Behav Brain Res* 2019, 373: 112079.
  44. Cao X, Li LP, Wang Q, Wu Q, Hu HH, Zhang M, *et al.* Astrocyte-derived ATP modulates depressive-like behaviors. *Nat Med* 2013, 19: 773–777.
  45. Kim SY, Adhikari A, Lee SY, Marshel JH, Kim CK, Mallory CS, *et al.* Diverging neural pathways assemble a behavioural state from separable features in anxiety. *Nature* 2013, 496: 219–223.
  46. Tye KM, Prakash R, Kim SY, Fenno LE, Grosenick L, Zarabi H, *et al.* Amygdala circuitry mediating reversible and bidirectional control of anxiety. *Nature* 2011, 471: 358–362.
  47. Felix-Ortiz AC, Burgos-Robles A, Bhagat ND, Leppla CA, Tye KM. Bidirectional modulation of anxiety-related and social behaviors by amygdala projections to the medial prefrontal cortex. *Neuroscience* 2016, 321: 197–209.
  48. Felix-Ortiz AC, Tye KM. Amygdala inputs to the ventral hippocampus bidirectionally modulate social behavior. *J Neurosci* 2014, 34: 586–595.
  49. Razzoli M, Andreoli M, Michielin F, de Quarta D, Sokal DM. Increased phasic activity of VTA dopamine neurons in mice 3 weeks after repeated social defeat. *Behav Brain Res* 2011, 218: 253–257.
  50. Bagot RC, Parise EM, Peña CJ, Zhang HX, Maze I, Chaudhury D, *et al.* Ventral hippocampal afferents to the nucleus accumbens regulate susceptibility to depression. *Nat Commun* 2015, 6: 7062.
  51. VanTieghem MR, Tottenham N. Neurobiological programming of early life stress: Functional development of amygdala-prefrontal circuitry and vulnerability for stress-related psychopathology. *Curr Top Behav Neurosci* 2018, 38: 117–136.